
Multiagent trajectory models via game theory and implicit layer-based learning

Philipp Geiger

Bosch Center for Artificial Intelligence

Christoph-Niklas Straehle

Bosch Center for Artificial Intelligence

Abstract

For prediction of interacting agents’ trajectories, we propose an end-to-end trainable architecture that hybridizes neural nets with game-theoretic principles, has interpretable intermediate representations, and transfers to robust downstream decisions. It combines a differentiable implicit layer, that maps preferences to local Nash equilibria, with a learned equilibrium refinement concept and preference revelation, upon initial trajectories as input. This is accompanied by a new class of continuous potential games, theoretical results for explicit gradients and soundness, and several measures to ensure tractability. In experiments, we evaluate our approach on two real-world data sets, where we predict highway driver merging trajectories, and a simple decision-making transfer task.

1 Introduction

For predicting interacting agents’ trajectories, data-driven approaches have yielded flexible, tractable, multi-modal methods, but it remains a challenge to use them for safety-critical domains with verification requirements, like automated driving. Towards addressing this challenge, the following seem sensible intermediate goals: (1) incorporation of well-understood *principles* and prior knowledge of the multiagent domain, that allow to generalize well, including transfer to robust downstream decision making, (2) *interpretability* of the model’s latent variables, allowing empirical verification beyond just testing the final output; (3) theoretical *analysis* for soundness.

In this paper, we address multiagent trajectory prediction with these additional goals, while trying to keep as much as possible of the strength of data-driven methods. For this, we hybridize neural nets with game theory, because game theory provides well-established explanations of agents’ behavior based on agents’ utilities and the principle of rationality (i.e., agents as utility maximizers). Along this hybrid direction, one major obstacle – and a general reason why game theory often remains in abstract settings – lies in classic game-theoretic solution concepts like the Nash equilibrium (NE) notoriously suffering from computational intractability. To overcome this obstacle, we built on recent developments in *local NE* [33, 34, 5]. We combine this with a specific class of games – (*continuous*) *potential games* [29] – for which local NE, roughly speaking, coincide with local optima of a single objective function, simplifying search. Another major challenge lies in combining game-theoretic principles with flexible neural nets in a way that makes the overall model still efficiently *trainable*. To address this, we build on the recent advancement of *implicit layers* [4, 11]. Implicit layers specify input-output relations not in closed form, but only implicitly through equations – a good match for local NE – while still getting exact gradients via the implicit function theorem.

Outline and main contributions. Our main contributions can be outlined as follows:

- In Sec. 3.1, we propose a new class of continuous-action trajectory games that allow to encode prior knowledge on agents’ utilities (Def. 4) and prove that they are potential games (Lem. 1). This induces a concave optimization-based implicit layer with explicit gradient formula, mapping game parameters to local Nash equilibria, thus encoding (a local version of) the principle of rationality

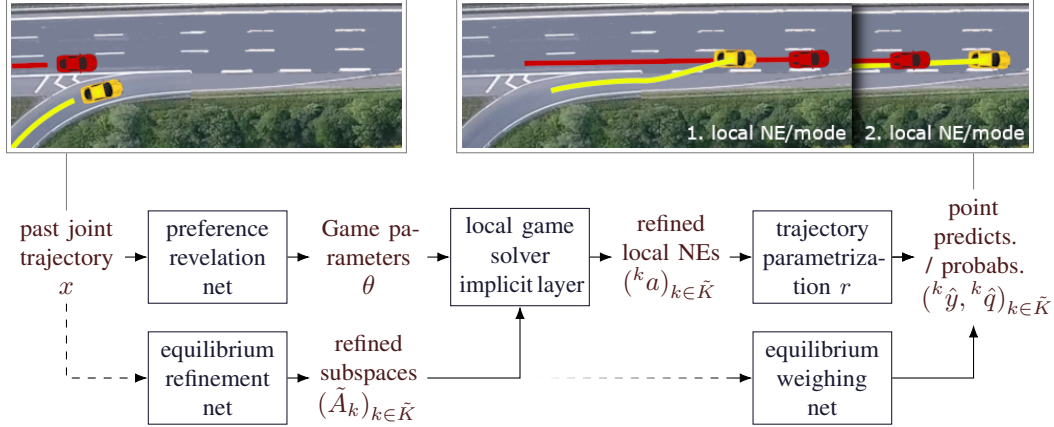


Figure 1: **Bottom:** Our full architecture (Sec. 3.2). **Top left:** example input x : initial trajectories of two drivers in highway entry merging scenario. **Top right:** example future trajectories y : depicted are *two modes* corresponding to *two local Nash equilibria* – red going first vs. yellow going first.

(Thm. 1). As a helpful tool for this, we use a form of “equilibrium-separating partition” of the action space (Def. 5).

- In Sec. 3.2, we propose a complete neural net architecture (Fig. 1 – with highway examples) that outputs a multi-modal trajectory prediction (where modes are interpretable as local Nash equilibria) based on a past trajectory segment as input. Besides the mentioned implicit layer, it contains a net that learns an equilibrium refinement concept (which, in particular, helps compensate the “locality relaxation” of NE), a “preference revelation net”, and several measures to make training tractable. This architecture forms a model class where certain hidden representations have clear game-theoretic interpretations and certain layers encode game-theoretic principles that help induction (also towards strategically-robust decision-making prescriptions), while at the same time having neural net-based capacity for learning, and the ability for analytic gradient-based training.
- In Sec. 4, we give two example scenarios that provably satisfy our approach’s conditions (Prop. 1,2).
- In the experiments reported in Sec. 5, we apply our approach to prediction of real-world highway on-ramp merging driver interaction trajectories, on one established and one new data set. We also apply it to a simple decision-making transfer task.

Now we first discuss related work and introduce setting and background (Sec. 2). Generally, proofs are in Sec. A.

Related work. Regarding general multiagent model learning from observational behavioral data with game-theoretic components: Closest related is work by Ling et al. [25, 26], who use game solvers as one differentiable implicit layer, also allowing to learn the input of this layer (i.e., agents’ preferences) from covariates. In contrast to us, they do not focus on trajectory prediction, in particular they only consider discrete actions. And they use (versions of) quantal response equilibria (QRE) instead of local NE, and do not consider equilibrium refinement. There is further work more broadly related in this direction [19, 20, 27, 18, 45, 23, 13, 8, 28, 43], sometimes also studying driver interaction scenarios, but they have no or little data-driven aspects (in particular no implicit layers) and/or use different, significantly simpler, approximations to rationality than our local NE, such as level- k reasoning, and often are less general than us, often focusing on discrete actions. More broadly related are multi-agent versions of inverse reinforcement learning [46, 35, 51, 1], usually discrete-action.

For multiagent trajectory prediction, there generally is a growing number of papers on the machine learning side, often building on deep learning principles and allowing multi-modality – but without game-theoretic components. Without any claim to completeness, there is work using long-short term memories (LSTMs) [2, 10, 39], generative adversarial networks (GANs) [14], and attention-based encoders [44]. Kuderer et al. [22] uses a partition (“topological variants”) of the trajectory space similar to ours. There is also work based on the principle of “social force” [17, 36, 6].

Regarding additional game-theoretic elements: W.r.t. the class of potential games we introduce (Def. 4), most closely related is Zazo et al. [48] who consider a related class of dynamic potential games (for control tasks), but they do not allow agents’ utilities to have differing additive terms w.r.t. their own actions. Related to this, worth mentioning is further work based on games (different ones than ours though) towards pure *control* (not prediction) tasks [32, 50, 41, 12]. Peters et al. [32] addresses control based on a latent variable for the equilibrium selection, similar to our equilibrium weighing. Noteworthy is also [16] who learn solution concepts, but not equilibrium refinement concepts.

2 General setting, predictive objective and background

General setting and predictive objective. We consider scenes where there is a set $I := \{1, \dots, n\}$ of agents. Each agent $i \in I$ at each time $t \in [0, T]$ has an *individual state* $y_t^i \in \mathbb{R}^{d_{y_i^i}}$. They yield an *individual trajectory* $y^i = (y_t^i)_{t \in [0, T]}$ (think of 0 as the present time point and T as the horizon up to which we want to predict). And $y := ((y_t^1, \dots, y_t^n))_{t \in [0, T]} \in Y$ denotes the agents’ *joint (future) trajectory*. We assume that the agents’ *past joint trajectory* x until time point 0 is available as side information. Now, besides the other goals mentioned in Sec. 1, our *predictive objective* is to output a list of pairs (\hat{y}, \hat{q}) , where \hat{y} is a point prediction and \hat{q} the associated probability, corresponding to the modes of y in a new scene, given past trajectory x of that scene, as well as samples of past and future trajectory from previous scenes (discrete-time subsampled of course).

We assume that agent i ’s (future) trajectory y^i is parameterized by a finite-dimensional vector $a^i \in A^i \subseteq \mathbb{R}^{d_{A^i}}$, which we refer to as i ’s *action*, with A^i the *action space*. So, in particular, there is a (joint) *trajectory parameterization* $r : A \rightarrow Y$, with $A := A^1 \times \dots \times A^n$ the *joint action space*. Keep in mind that a^{-i} means $(a^1, \dots, a^{i-1}, a^{i+1}, a^n)$ and (a^i, a^{-i}) reads a .

We use games [40, 31, 30] to model our setting. A game specifies the set of agents (also called “players”), their possible actions and their utility functions. The following formal definition is slightly adapted to our setting, such that utilities are integrals over the trajectories parameterized by the actions:

Definition 1 ((Trajectory) game). *A (trajectory) game consists of: the set I of agents, and for each agent $i \in I$: the action space $A^i \subseteq \mathbb{R}^{d_{A^i}}$, and a utility function $u^i : A \rightarrow \mathbb{R}$. We assume $u^i, i \in I$, to be of the form $u^i(a) = \int_0^T u_t^i(y_{[t-\Delta, t]}) d\mu(t)$, $a \in A$, where $u_t^i, t \in [0, T]$, are the stage-wise utility functions, $y = r(a)$, μ is a measure on the time, and $y_{[t-\Delta, t]}$ reads $(y_t)_{t \in [t-\Delta, t]}$, for some $\Delta \geq 0$.^{1 2}*

Now while a game essentially formalizes the agents’ decision-making “*problem*”, let us also introduce a (local kind of) concept that formalizes how agents will/should act to “*solve*” the game:

Definition 2 (Local Nash equilibrium [34, 33, 5]). *Given a game, a joint action $a \in A$ is a (pure) local Nash equilibrium (NE) if there are open sets $S_i \subset A^i$ such that, for each i , $a_i \in S_i$ and $u^i(a^i, a^{-i}) \geq u^i(a^{i'}, a^{-i})$ for any $a^{i'} \in S_i$. If the above inequality is strict, we call a a strict (pure) local Nash equilibrium. If $S_i = A_i$ for all i , then a is a (pure, global) Nash equilibrium.*

The following type of game will be useful for us, in particular for tractability reasons.

Definition 3 (Potential game [29, 37]). *A game is called an (exact continuous) potential game, if there is a so-called potential function ψ such that $u^i(a^{i'}, a^{-i}) - u^i(a^i, a^{-i}) = \psi(a^{i'}, a^{-i}) - \psi(a^i, a^{-i})$, for all agents i , all actions $a^i, a^{i'}$ and remaining actions a^{-i} .*

Background on implicit layers. Classical neural layers specify the functional relation between an input v and an output w *explicitly*, in some closed form $w = f(v)$. The idea of implicit layers [4, 11, 9, 3] is to specify the relation *implicitly* via an equation, say $h(v, w) = 0$. To ensure that this specification is indeed useful in prediction and training, two things are important: (1) the equation determines a unique (tractable) function g that maps v to w , and (2) g is differentiable, ideally with explicitly given analytic gradients.

¹To keep it flexible, we use an integral-based formulation, but an important special case (Scenario 1) will be discrete-time, with μ ’s mass on discrete time points. We use subscript $[t - \Delta, t]$ to allow dependence on, say, velocity.

²For tractability/analysis reasons we consider this simple deterministic form instead of, say, a Markov game.

3 General approach: game, architecture and analysis

We now describe our general approach. It consists of a class of games with induced implicit layer and analysis (Sec. 3.1). This together with additional modules forms a complete neural net architecture, with tractable training and decision-making transfer abilities (Sec. 3.2).

3.1 Common-coupled game, maximum-separation, and induced implicit layer

Let $(\Gamma_\theta)_{\theta \in \Theta}$, $\Theta \subseteq \mathbb{R}^{d_\Theta}$, be a parametric family of games. We introduce the following type of game as a tractable model of many multiagent trajectory settings, especially those with (implicit) social norms and/or common interests (say, not crashing) that agents trade off against personal inclinations. It is non-cooperative, i.e., utilities differ, but more on the cooperative than adversarial end of games.

Definition 4 (Common-coupled game). *We call Γ_θ a common-coupled(-term trajectory) game , if the stage-wise utility function (Def. 1) of agent i has the following form:*

$$u_t^{i,\theta}(y_{[t-\Delta,t]}) = u_t^{\text{com},\theta}(y_{[t-\Delta,t]}) + u_t^{\text{own},i,\theta}(y_{[t-\Delta,t]}^i) + u_t^{\text{oth},i,\theta}(y_{[t-\Delta,t]}^{-i}), \text{ for all } t \in [0, T], \quad (1)$$

where $y = r(a)$ (action parameterizes trajectory, Sec. 2), $u_t^{\text{com},\theta}$ is a term that depends on all agents' trajectories and is common between agents, $u_t^{\text{own},i,\theta}$ and $u_t^{\text{oth},i,\theta}$ are terms that only depend on agent i 's trajectory, or all other agents' trajectories, respectively, and (may) differ between agents.

Lemma 1. *If Γ_θ is a common-coupled game, then it is a potential game with the following potential function: $\psi(a, \theta) = \int_0^T u_t^{\text{com},\theta}(y_{[t-\Delta,t]}) + \sum_{i \in I} u_t^{\text{own},i,\theta}(y_{[t-\Delta,t]}^i) d\mu(t)$, where, as usual, $y = r(a)$.*

Note that this implies existence of NE, given continuity of the utilities and compactness [29]. The following definition – whenever the game permits it – will be a simple but versatile tool for the implicit layer and for tractability. Let $(\tilde{A}_k)_{k \in K}$ be a collection of subspaces of A , i.e., $\tilde{A}_k \subseteq A$.

Definition 5 (Maximum-separating action subspaces). *For a common-coupled game Γ_θ , we call the action subspace collection $(\tilde{A}_k)_{k \in K}$ maximum-separating if, for all $k \in K$ and $\theta \in \Theta$, its potential function $\psi(\theta, \cdot)$ is strictly concave on \tilde{A}_k .³*

Assumption 1. *Let Γ_θ be a common-coupled game. Let $(\tilde{A}_k)_{k \in K}$ be maximum-separating subspaces for it, and let all $\tilde{A}_k, k \in K$ be compact, given by the intersection of linear inequality constraints. On each subspace $\Theta \times \tilde{A}_k, k \in K$, let Γ_θ 's potential function ψ be continuous.*

Theorem 1 (Game-induced differentiable implicit layer). *Let Assumption 1 hold true. Then, for each $k \in K$, there is a continuous mapping $g_k : \Theta \rightarrow \tilde{A}_k$, such that, if $g(\theta)$ lies in the interior of \tilde{A}_k , then $g_k(\theta)$ is a local NE of Γ_θ and*

- $g_k(\theta)$ is given by the unique argmax (tractably solvable due to concavity) of $\psi(\theta, \cdot)$ on \tilde{A}_k , with ψ the game's potential function (Lem. 1),
- g_k is continuously differentiable in θ with gradient $J_\theta g_k(\theta) = -(H_a \psi(\theta, a))^{-1} J_\theta \nabla_a \psi(\theta, a)$, given ψ is twice continuously differentiable on (an open set containing) (θ, a) , for $a = g_k(\theta)$, where ∇, J and H denote gradient, Jacobian and Hessian, respectively.

In what follows, by default, under Assumption 1, as the (induced) local game solver implicit layer we consider $g := (g_1, \dots, g_{|\tilde{K}|})$, i.e., the mapping that gives the local NE within $(\tilde{A}_k)_{k \in \tilde{K}}$, given any $\tilde{K} \subseteq K$.

Remark on boundaries. There remain several questions: e.g., whether the action subspacing introduces “artificial” local NE at the boundaries of the subspaces; and also regarding what happens to the gradient if $g_k(\theta)$ lies at the boundary of A or \tilde{A}_k . While we have several simple results for these questions, for space reasons we restrict to stating the following partial answer to the latter:

³To have a rough intuition, think of $(\tilde{A}_k)_{k \in K}$ as a partition of (a subset of) A , but we allow overlaps. The subspaces also have the interpretation as macroscopic/high-level joint action of the agents: for instance, which car goes first in the merging scenario in Fig. 1.

Lemma 2. *Let Assumption 1 hold true and additionally assume ψ to be continuously differentiable on (a neighborhood of) $\Theta \times \tilde{A}_k, k \in K$. If $a = g_k(\theta)$ lies on (exactly) one constraining hyperplane of \tilde{A}_k , defined by orthogonal vector v , with multiplier λ and optimum $\lambda^* > 0$ of $\psi(\theta, a)$'s Lagrangian (details in the proof), then $J_\theta g_k(\theta) = \left[- \begin{pmatrix} H_a \psi(\theta, a) & v \\ \lambda^* v^T & 0 \end{pmatrix}^{-1} \begin{pmatrix} J_\theta \nabla_a \psi(\theta, a) \\ 0 \end{pmatrix} \right]_{1:(n \cdot d_{A1}) \times 1:(n \cdot d_{A1})}$.*

Remark on identifiability. Another natural question is whether the game's parameters are *identifiable* from observations – and, especially, whether g is invertible. While not the main scope of the paper, and difficult to answer in general, we will investigate this for one scenario below (Prop. 2).

3.2 Full architecture with further modules, tractable training, and decision making

Full architecture. We propose the architecture depicted in Fig. 1 calling it *trajectory game learner (TGL)*. Besides the local game solver implicit layer just described (Sec. 3.1) it contains the following modules: The *preference revelation net* maps the initial joint trajectory x to game parameters θ .⁴ The *equilibrium refinement net* learns a game-theoretic “equilibrium refinement concept” to narrow down the set of local NE.⁵ For tractable training reasons (see Sec. 3.2), we use a trick: instead of directly outputting a subset of equilibria, we output a subcollection $(\tilde{A}_k)_{k \in \tilde{K}}$ of a maximum-separating action subspace collection $(\tilde{A}_k)_{k \in K}$, determining a refined set $({}^k a)_{k \in \tilde{K}}$ of local NE. The *equilibrium weighing net* outs probabilities $({}^k \hat{q})_{k \in \tilde{K}}$ over the equilibria (that remain after refinement), i.e., modes of our forecast. This can be seen as (probabilistically) learning agents’ “equilibrium selection” mechanism considered in game theory.⁶

For concrete examples of the neural nets see Sec. 5. Regarding input and function class for equilibrium refinement and weighing net, in principle one can think of many combinations of y, θ, a , and function classes. Here, for the sake of our tractable training approach (details below), we only allow the equilibrium refinement to depend on x or θ , so the dashed arrows in Fig. 1 indicate possible inputs.

Training and tractability. Note that the full architecture is *not* differentiable, because the equilibrium refinement net’s output is discrete. However, it is easy to see that (1) the equilibrium refinement net and (2) the rest of the architecture can be trained *separately*: in training, for each sample (x, y) , we directly know which subspace y lies in, so we simply deploy the local game solver on this subspace. On a related note, we learn the common term’s parameter θ (see (1)) as shared between all scenes, while the other parameters are predicted from the individual’s sample past trajectory.

Also observe that in training there is an outer (parameter fitting) and an inner (game solver, i.e., potential function maximizer, during forward pass) optimization loop, so their speed is crucial. For the game solver, we recommend quasi-Newton methods like L-BFGS, because this is possible due to the subspace-wise concavity of the potential function (Assumption 1). For the outer loop, we recommend recent stochastic quasi-Newton methods [47, 24] with the explicit gradient from Thm. 1.

Downstream decision making. Once the (common-coupled) game Γ_θ including parameters θ is learned (for arbitrary numbers of agents), we can use this model also for *prescriptive* purposes: i.e., how a newly introduced agent *should* decide to maximize its utility, while aware of the strategic other agents modeled by Γ_θ (think of a self-driving car entering a scene with other human drivers). This is due to the double nature of game theory: predictive and prescriptive. Note though that what the knowledge of Γ_θ cannot resolve is the remaining equilibrium selection problem (but sometimes the equilibrium weighing net can be applied). For an example see Sec. 5.2.

⁴In a sense, this net is the inverse of the game solver implicit layer on x , but can be more flexible.

⁵In game theory, “equilibrium refinement concepts” mean hand-crafted concepts that further narrow down the set of (Nash) equilibria of a game (for various reasons, such as achieving more “stable” solutions) [40, 31]. For us, an important purpose is also tractability – because sometimes the set of local Nash equilibria can grow almost exponentially in the number of agents.

⁶“Equilibrium selection” [15] refers to the problem of which *single* equilibrium agents will end up choosing if there are multiple – possibly even after a refinement.

4 Two example scenarios with analysis

Let us give two examples of settings alongside games and action subspace collections that provably fulfill the conditions for our general approach (Sec. 3) to apply.

4.1 Multi-lane driver interaction

First we consider a scenario which captures various non-trivial driver interactions like overtaking or merging at on-ramps. Essentially, it consists of a straight (or slightly bent) road section with multiple (same-directional) lanes, where some lanes can end within the section (Fig. 1 is an example). The implicit layer induced by this setting will be used in the experiments (Sec. 5).

Scenario 1 (Multi-lane driver interaction). **Setting:** *The set of possible individual states, denote it by Y_0 , is of the form $[b, c] \times [d, e]$ – positions on a road section. There are m parallel lanes (some of which may end), parallel to the x -axis. Agent i 's action $a^i \in A^i$ is given by the sequence of planar (i.e., 2-D) positions denoted $(v_t^i, w_t^i) \in Y_0 \times Y_0, t = 0, \dots, T$, but not allowing backward moves (and possibly other constraints). The trajectory y^i is the linear interpolation. **Game:** Let, for $t = 0, \dots, T$, the stage utilities of agent i in the game Γ_θ be the following sum of terms for distance between agents, distance to center of lane, desired velocities, acceleration penalty, and distance to end of lane overshooting penalty, respectively:⁷*

$$u_t^{i,\theta}(y_{[t-2,t]}^i) = -\theta^{dist} \sum_{j \text{ right before } j' \text{ on same lane}} \frac{1}{|v_t^j - v_t^i| + \zeta} - \theta^{cen,i} (w_t^i - c_t^i)^2 \quad (2a)$$

$$- \theta^{vel,i} (\delta v_t^i - \theta^{v,i})^2 - \theta^{velw,i} (\delta w_t^i)^2 - \theta^{acc,i} (\delta^2 v_t^i)^2 - \theta^{end,i} \max(0, v_t - e_t), \quad (2b)$$

where $\zeta > 0$ is a constant, c_t^i is the respective center of the lane, δv_t^i means velocity along lane, $\delta^2 a_t^i$ means acceleration (vector), e_t is the end of the lane, if it ends, otherwise $-\infty$; furthermore, μ is the counting measure on $\{0, \dots, T\}$ (i.e., discrete), and $\Delta = 2$. **Subspaces:** Consider the following equivalence relation on the trajectory space Y : two joint trajectories $y, y' \in Y$ are equivalent if at each time point t , (1) each agent i is on the same lane in y as in y' , and (2) within each lane, the order of the agents (along the driving direction) is the same in y as in y' . Now let the subspace collection $(\tilde{A}_k)_{k \in K}$ be obtained by taking the equivalence classes from this eq. relation.

Proposition 1 (Scenario 1's suitability). *Scenario 1 satisfies Assumption 1. So, in particular, Thm. 1's implications on the induced implicit layer hold true.*

4.2 Simple pedestrian encounter

When considering settings with characteristics such as continuous time, even if they still satisfy the conditions of our framework, to prove so can become arbitrarily complex. Here let us give a simplistic but verified second example with properties somewhat different from the first one: Consider two pedestrians who walk with constant speed along straight paths which are orthogonal and intersect such that they could bump into each other (Fig. 2). Formally:

Scenario 2 (Simple pedestrian encounter). **Setting:** *There are $n = 2$ agents, the actions parameterize the trajectories via $y_t^1 = (0, ta^1 + z^1)$, $y_t^2 = (ta^2 + z^2, 0)$ (for ease of notation, we put the intersection to the origin but translations are possible of course), the joint action space is $A = [\frac{z^1}{T}, c] \times [\frac{z^2}{T}, c]$, for constants $z^1, z^2 < 0$ and $c > 0$, (the lower bound on the action is to make sure they reach the intersection). **Game:** Let the final stage utility be given by the following sum of a distance penalty term and a desired velocity term*

$$u_T^{i,\theta}(y_{[0,T]}^i) = -h(\theta^{dist}, a) \max_{t \in [0,T]} \frac{1}{\|y_t^1 - y_t^2\|_1} - \theta^{vel,i} (a^i - \theta^{v,i})^2 (= -\infty \text{ if division by } 0), \quad (3)$$

for some function h , $\theta^{vel,i} > 0$, and let μ be the Dirac measure on T , and $\Delta = T$ (We use this terminal-term and Dirac delta-based formulation to properly fit it into the general Def. 1). **Subspaces:** Let the

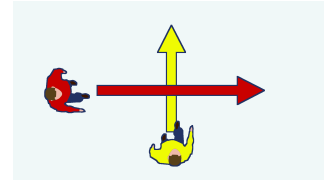


Figure 2: Simple pedestrian encounter.

⁷Note that the invariance over time of the utility terms, as we assume it here, is a key element of how rationality principles can give informative priors.

subspaces $(\tilde{A}_k)_{k \in K}$ be given by (1) taking the two subspaces that satisfy $a_k \geq a_{2-k} + \varepsilon$, for $k = 1, 2$ respectively, and some small $\varepsilon > 0$, i.e., split by which agent is faster, and (2) additionally split by which agent first reaches their paths’ intersection (altogether this yields two or three subspaces).

Proposition 2 (Scenario 2’s suitability and partial identifiability). *Assume Scenario 2 with $h(\theta^{dist}, a) = \frac{1}{a_k}$, with k being the faster agent in a . Then Assumption 1 is satisfied. Furthermore, while the complete game parameter $\theta = (\theta^{vel,1}, \theta^{v,1}, \theta^{vel,2}, \theta^{v,2}, \dots)$ is not identifiable in general, if $\theta^{vel,i}, i = 1, 2$ is constant, then $(\theta^{v,1}, \theta^{v,2})$ is identifiable from y on the pre-image of the interior of \tilde{A}_k , for any k .*

5 Experiments

We evaluate our approach on (1) a prediction task on two real-world data sets (Sec. 5.1), as well as (2) a simple decision-making transfer task (Sec. 5.2).

5.1 Prediction task on highway merging scenarios in two real-world data set

We consider a highway merging interaction scenario with two cars, one on the on-ramp, and one nearby on the rightmost lane of the highway, similar as sketched in Fig. 1.

Implementation details for our method for these merging scenario. We use our general approach (Sec. 3), with Scenario 1 ($n = 2$) as game and a smart parameterization of the actions to avoid constraints. We use validation-based early stopping. We combine equilibrium refinement and weighing net into one simple feed forward NN (1×64 neurons, dropout 0.6) that predicts the weights $({}^k \hat{q})_{k \in \tilde{K}}$ on the combination of (1) merging order (before/ after) probabilities via a cross-entropy loss and (2) Gaussian distribution over merging time point (where we discretize and truncate the latter, thus the support inducing a refinement), given x . For the preference revelation net we use a simple feed forward NN (2×16 neurons). For larger data sets and varying initial trajectory lengths, an LSTM might be more suitable. As training loss we use MAE. Besides this method – TGL – we also use a version of it – termed *TGL-P* – for which we use the interpretable representation of the desired velocity parameter predicted by the preference revelation net, which we first validate, and then encode *prior-knowledge based constraints* (e.g., we clip maximum and minimum desired speed). Note that this prior knowledge of course may not always be easy to specify and depends on the situation. For details on TGL-P, see Sec. B.

Baseline. As baseline we use the state-of-the-art data-driven method “convolutional social pooling” – specifically: *CS-LSTM* [10] – for which code was available on the web⁸. **Evaluation.** We use four-fold cross validation (splitting the training set into 67% train and 33% validation). As metrics, we use rooted mean squared error (RMSE) and mean absolute error (MAE) averaged over a 7s horizon with prediction step size of 0.2s, applying this to the most likely mode given by our method.

Data sets – including a new one published alongside the paper – and filtering: *First data set:* We use the “highD” data set [21], which consists of car trajectories recorded by drones that flew over several highway sections. It is rather new but increasingly used for benchmarking [38, 49]. From this data set, we use the recordings done over a section with an on-ramp. *Second data set:* We publish a new data set along this paper with several types of highway driver interaction types – besides the merging scenario. It consists of ~ 12000 individual car trajectories (~ 3.5 h), recorded by drones that flew over one highway section with an entry lane (see supplement). Fig. 1 shows a stylized – significantly squeezed – partial picture of the recorded highway section. *Selection of merging scenes in both data sets:* We filter for all joint trajectories of two cars where one is merging, one is on the highway, and all other cars are far enough to not interact with these two. This leaves 25 trajectories of highD and 23 of our new data set.

Results. The results are in Table 1, with more details in the supplement. Our general method TGL outperforms CS-LSTM on highD. And our method TGL-P additionally is essentially on par with CL-LSTM on our new data set. Keep in mind that we do not solely aim at prediction performance,

⁸Another state-of-the-art [44] method’s code became publicly available just shortly before submission.

Data set	Metric	TGL (ours)	TGL-P (ours)	CS-LSTM [10]
highD [21]	MAE	3.7	2.5	5.0
	RMSE	5.4	3.5	6.8
New data set (Sec. 5.1)	MAE	3.8	3.4	3.5
	RMSE	5.0	4.9	4.2

Table 1: Our method(s) vs. state-of-the-art for a prediction task on two real-world highway merging data sets, averaged over a 7s prediction horizon.

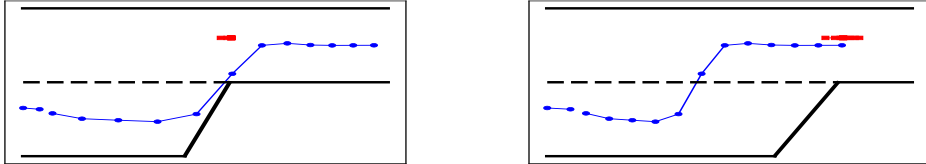


Figure 3: Solution trajectory(s) that the learned game implies for the self-driving car’s decision-making task (each circle/square corresponds to one time step). *Left*: First local NE – the self-driving car (red) does a full emergency break and the other (blue) merges before it. *Right*: The other local NE – the other merges after it, both slow down.

but, as stated in the introduction, also aim at principled transferability/ interpretability – which often requires a trade-off to purely predictive metrics.

5.2 Simple decision-making task

As already discussed in Sec. 3.2 the game Γ_θ – once θ is given, e.g., by our learned preference revelation net – naturally transfers to decision-making tasks in situations with multiple strategic agents (something which predictive methods like the above CS-LSTM usually cannot do). To test and illustrate its ability for this, we consider a simple scenario: Take the above two-car highway on-ramp situation (based on Scenario 1), but assume that the car on the rightmost highway lane, refer to it as ego car, is a self-driving car. Assume it has a technical failure roughly at the height of the end of the on-ramp, and it would be important to stop (i.e., desired velocity $\theta^{v,i}$ in (2) is set to 0), while at the same time its objective is to ensure that the other car coming from the on-ramp will keep a safe distance and does not crash into it. (Assume it cannot stir towards the side track.) Which trajectory should it choose? **Result.** Fed with this situation, our game solver suggests two possible solutions – two local NE, see Fig. 3: (1) the ego car completely stops and the on-ramp car will merge after it, accepting to shoot over the on-ramp’s end (2) the ego car moves slowly, but at a non-zero speed, with the other car right behind it. While a toy scenario, we feel that these are realistic solutions.

6 Conclusion

We proposed an end-to-end trainable model class for multiagent trajectories. It integrates descriptions of the underlying mechanism in the form of interpretable game-theoretic principles and knowledge, while at the same time being able to flexibly learn from observed trajectories using neural nets. A major challenge was to make game-theoretic concepts practically applicable for this setting. Towards addressing this, we built on local Nash equilibria and implicit layers, accompanied by theoretical analysis. In experiments on two real-world data sets, we demonstrated the practicality and prediction performance for highway merging, and showed, in contrast to most classical predictive methods, the built-in ability to transfer to decision-making tasks. We think this is a meaningful direction towards verified safety in such scenarios.

Acknowledgments: We thank Jalal Etesami for insightful discussions and the anonymous reviewers for their hints.

Appendix

A Proofs and remarks

A.1 Lemma 1

Let us first restate the result.

Lemma 1. *If Γ_θ is a common-coupled game, then it is a potential game with the following potential function: $\psi(a, \theta) = \int_0^T u_t^{\text{com}, \theta}(y_{[t-\Delta, t]}) + \sum_{i \in I} u_t^{\text{own}, i, \theta}(y_{[t-\Delta, t]}^i) d\mu(t)$, where, as usual, $y = r(a)$.*

Proof of Lemma 1. Recall that based on the definition of a common-coupled game we have have for the stage-wise utility for all i and t ,

$$u_t^{i, \theta}(y_{[t-\Delta, t]}) = u_t^{\text{com}, \theta}(y_{[t-\Delta, t]}) + u_t^{\text{own}, i, \theta}(y_{[t-\Delta, t]}^i) + u_t^{\text{oth}, i, \theta}(y_{[t-\Delta, t]}^{-i}). \quad (4)$$

Now observe that for all i and t ,

$$\begin{aligned} & u_t^{i, \theta}((y_{[t-\Delta, t]}^{i'}, y_{[t-\Delta, t]}^{-i})) - u_t^{i, \theta}((y_{[t-\Delta, t]}^i, y_{[t-\Delta, t]}^{-i})) \\ &= u_t^{\text{com}, \theta}((y_{[t-\Delta, t]}^{i'}, y_{[t-\Delta, t]}^{-i})) - u_t^{\text{com}, \theta}((y_{[t-\Delta, t]}^i, y_{[t-\Delta, t]}^{-i})) \\ &+ u_t^{\text{own}, i, \theta}(y_{[t-\Delta, t]}^{i'}) - u_t^{\text{own}, i, \theta}(y_{[t-\Delta, t]}^i) + 0 \\ &= u_t^{\text{com}, \theta}((y_{[t-\Delta, t]}^{i'}, y_{[t-\Delta, t]}^{-i})) - u_t^{\text{com}, \theta}((y_{[t-\Delta, t]}^i, y_{[t-\Delta, t]}^{-i})) \\ &+ u_t^{\text{own}, i, \theta}(y_{[t-\Delta, t]}^{i'}) - u_t^{\text{own}, i, \theta}(y_{[t-\Delta, t]}^i) + \sum_{j \in I \setminus i} u_t^{\text{own}, j, \theta}(y_{[t-\Delta, t]}^j) - \sum_{j \in I \setminus i} u_t^{\text{own}, j, \theta}(y_{[t-\Delta, t]}^j). \end{aligned}$$

Integrating w.r.t. t and using the linearity of the integral completes the proof. □

A.2 Theorem 1

Let us first restate the result.

Theorem 1 (Game-induced differentiable implicit layer). *Let Assumption 1 hold true. Then, for each $k \in K$, there is a continuous mapping $g_k : \Theta \rightarrow \tilde{A}_k$, such that, if $g(\theta)$ lies in the interior of \tilde{A}_k , then $g_k(\theta)$ is a local NE of Γ_θ and*

- $g_k(\theta)$ is given by the unique argmax (tractably solvable due to concavity) of $\psi(\theta, \cdot)$ on \tilde{A}_k , with ψ the game's potential function (Lem. 1),
- g_k is continuously differentiable in θ with gradient $J_\theta g_k(\theta) = -(H_a \psi(\theta, a))^{-1} J_\theta \nabla_a \psi(\theta, a)$, given ψ is continuously differentiable on (an open set containing⁹) (θ, a) , for $a = g_k(\theta)$, where ∇ , J and H denote gradient, Jacobian and Hessian, respectively.

Proof of Theorem 1.

Gradient etc. Based on Lemma 1, the potential function ψ exists. Let $k \in K$ be arbitrary but fixed. Let g_k be the function that maps each θ to the corresponding unique maximum of $\psi(\theta, \cdot)$ on \tilde{A}_k (exists and is unique by the assumption of strict concavity and convexity and compactness of the \tilde{A}_k). From the definition of the potential function and the local Nash equilibrium (NE), it follows directly that a maximum of the potential function is a local NE of the game.

To apply the implicit function theorem, let us consider the point $(\theta, g_k(\theta))$. If the minimum $g_k(\theta)$ lies in the interior of \tilde{A}_k , and ψ is continuously differentiable on an open set containing $(\theta, g_k(\theta))$, then we have $\nabla_a \psi(\theta, a)|_{(\theta, a)=(\theta, g_k(\theta))} = 0$ and furthermore, by assumption of strict concavity, $J_a \nabla_a \psi(\theta, a)|_{(\theta, a)=(\theta, g_k(\theta))}$ non-singular. Then the implicit function theorem implies that there is a

⁹NB: This we added compared to the main text's submitted version.

an open set O containing $(\theta, g_k(\theta))$, and a unique continuously differentiable function $f : O \rightarrow \tilde{A}_k$, such that $\nabla_a \psi(\theta', f(\theta')) = 0$ for $\theta' \in O$, with gradient

$$J_\theta f(\theta) = -(J_a \nabla_a \psi(\theta, a))^{-1} J_\theta \nabla_a \psi(\theta, a) = -(H_a \psi(\theta, a))^{-1} J_\theta \nabla_a \psi(\theta, a). \quad (5)$$

Now on O , f and g_k coincide since f is uniquely determined (specifically, based on the implicit function theorem, locally, the graph of f coincides with the solution set of $\nabla_a \psi(\cdot, \cdot) = 0$, and if f, g_k would differ in at least one point θ' , then there would be a solution $(\theta', g_k(\theta'))$ outside the solution set – a contradiction). Therefore g_k is also continuously differentiable on O with gradient

$$J_\theta g_k(\theta) = J_\theta f(\theta). \quad (6)$$

We can do this for every θ , which completes the proof.

Continuity. Since ψ is continuous, \tilde{A}_k is compact, and the maxima are unique, the *maximum theorem* implies that the mapping g_k is in fact continuous (hemicontinuity reduces to continuity when the correspondence is in fact a function). □

A.3 Lemma 2 with remark on zero gradient

Let us first restate the result.

Lemma 2. *Let Assumption 1 hold true and additionally assume ψ to be continuously differentiable on (a neighborhood of) $\Theta \times \tilde{A}_k, k \in K$. If $a = g_k(\theta)$ lies on (exactly) one constraining affine¹⁰ hyperplane of \tilde{A}_k , defined by orthogonal vector v , with multiplier λ and optimum $\lambda^* > 0$ of $\psi(\theta, a)$'s Lagrangian (details in the proof), then $J_\theta g_k(\theta) =$*

$$\left[- \begin{pmatrix} H_a \psi(\theta, a) & v \\ \lambda^* v^T & 0 \end{pmatrix}^{-1} \begin{pmatrix} J_\theta \nabla_a \psi(\theta, a) \\ 0 \end{pmatrix} \right]_{1:(n \cdot d_{A^1}) \times 1:(n \cdot d_{A^1})}.$$

Remark on zero gradient. Note that under the conditions of this lemma, i.e., when $g_k(\theta)$ lies at the boundary, then the above gradient $J_\theta g_k(\theta)$ in fact often becomes zero, which can be a problem for parameter fitting. So the above result is only meant as a first step.

Proof of Lemma 2. Let \tilde{A}_k be defined by the inequality constraints $v_m^T a \leq b, m = 1, \dots, M$. Consider the Lagrangian

$$\Lambda(\theta, a, \lambda_1, \dots, \lambda_M) = \psi(\theta, a) + \sum_m \lambda_m (v_m^T a - b).$$

Then the Karush-Kuhn-Tucker optimality conditions [7] (note that we assumed differentiability of ψ on a neighborhood of $\Theta \times \tilde{A}_k, k \in K$) include the following equations:

$$\nabla_a \Lambda(\theta, a, \lambda_1, \dots, \lambda_M) = 0, \quad (7a)$$

$$\lambda_m (v_m^T a - b) = 0, \quad m = 1, \dots, M. \quad (7b)$$

Now let $a^* = g_k(\theta)$ and let $\lambda_1^*, \dots, \lambda_M^*$ be the (optimal) duals for a^* . And assume that a^* lies on exactly one bounding (affine) hyperplane. W.l.o.g. let this hyperplane correspond to v_1, λ_1^* . Also recall that g_k is continuous (as in Theorem 1). Therefore, in a neighbourhood of θ , the corresponding optimum will not lie within any of the other boundaries. So in this neighbourhood of θ , all corresponding optimal duals will be zero (inactive) except for the assumed one.

Therefore, given a θ' from the mentioned neighborhood of θ , we have that a, v_1 satisfy the optimality conditions in (7) (for some remaining duals) iff they satisfy the reduced conditions

$$\nabla_a \Lambda(\theta', a, \lambda_1, \lambda, 0, \dots, 0) = 0, \quad (8a)$$

$$\lambda_1 (v_1^T a - b) = 0. \quad (8b)$$

¹⁰This ‘‘affine’’ was missing in the main text.

For succinctness, in what follows we write λ instead of λ_1 , i.e., drop the subscript. Let

$$\begin{aligned} h(\theta', a, \lambda) &:= (\nabla_a \Lambda(\theta', a, \lambda, 0, \dots, 0), \lambda(v^T a - b)) \\ &= (\nabla_a \psi(\theta', a) + \nabla_a \lambda(v^T a - b), \lambda(v^T a - b)) \\ &= (\nabla_a \psi(\theta', a) + \lambda v^T, \lambda(v^T a - b)) \end{aligned}$$

So the conditions in (8) are

$$h(\theta', a, \lambda) = 0. \quad (9)$$

Similar as in Theorem 1, around the point $\theta, a^*, \lambda^*, g_k$ satisfies (9) (for some λ 's). So we can apply the implicit function theorem to get its gradient.

We have

$$\begin{aligned} &J_{(\theta, a, \lambda)} h(\theta, a, \lambda) \\ &= \begin{pmatrix} J_\theta \psi(\theta, a) & H_a \psi(\theta, a) & v^T \\ 0 & \lambda v^T & v^T a - b \end{pmatrix}. \end{aligned}$$

Note that

$$\begin{pmatrix} H_a \psi(\theta, a^*) & v^T \\ \lambda^* v^T & v^T a^* - b \end{pmatrix} = \begin{pmatrix} H_a \psi(\theta, a^*) & v^T \\ \lambda^* v^T & 0 \end{pmatrix}$$

is invertible, since

$$\det \left(\begin{pmatrix} H_a \psi(\theta, a^*) & v^T \\ \lambda^* v^T & 0 \end{pmatrix} \right) = \det(H_a \psi(\theta, a^*)) \det(-\lambda^* v^T (H_a \psi(\theta, a^*))^{-1} v)$$

and both factors are non-zero since $H_a \psi(\theta, a^*)$ is positive definite and λ^*, v are non-zero.

Therefore, the implicit function theorem is applicable to the equation, and we get as gradient

$$J_\theta g_k(\theta) = - \begin{pmatrix} H_a \psi(\theta, a^*) & v^T \\ \lambda^* v^T & 0 \end{pmatrix}^{-1} \begin{pmatrix} J_\theta \psi(\theta, a^*) \\ 0 \end{pmatrix}$$

□

A.4 Proposition 1

Let us first restate the result.

Proposition 1 (Scenario 1's suitability). *Scenario 1 satisfies Assumption 1. So, in particular, Thm. 1's implications on the induced implicit layer hold true.*

Proof of Proposition 1.

Common-coupled game. It is directly clear from the form of the utilities in Scenario 1, that this forms a common-coupled game.

Strict concavity of the potential function. Observe that, for each i , within any one subspace \tilde{A}_k , for each t ,

- i does not changes lane, so c_t, e_t are simple constants.
- For each lane, there is a fixed set of agents. Consider the set S of pairs (j, j') of agents that are on this lane and j is right before j' . This ordering (and thus S) is invariant within \tilde{A}_k . Therefore the agent distance term can be rewritten like

$$\theta^{\text{dist}} \sum_{j \text{ right before } j' \text{ on same lane}} \frac{1}{|v_t^j - v_t^{j'}| + \zeta} \quad (10)$$

$$= \theta^{\text{dist}} \sum_{(j, j') \in S} \frac{1}{v_t^{j'} - v_t^j + \zeta} \quad (11)$$

So all terms are concave, therefore the overall potential function, which is just a sum of them, is concave.

Futhermore, note that the sum of all velocity and distance to lane center terms is a sum of functions such that for each component of the vector a there is exactly one function of it, and only of it; and each function is strictly concave. This implies that the overall sum is strictly concave in the whole a . So the potential function is a sum of concave and a strictly concave term, meaning it is strictly concave.

NB: On the subspaces, the potential function is also differentiable.

Compactness and linearity of constraints. Besides the constraints that define the compact complete action space A , which are obviously linear, the constraints that define the action subspaces \tilde{A}_k are given by the intersection of constraints for each time point t that are all of the form

- $w_t^i \geq \text{const.}$ or $w_t^i \leq \text{const.}$, or
- $v_t^i \leq v_t^j$,

so they are linear. □

A.5 Proposition 2

Let us first restate the result.

Proposition 2 (Scenario 2's suitability and partial identifiability). *Assume Scenario 2 with $h(\theta^{dist}, a) = \frac{1}{a_k}$, with k being the faster agent in a . Then Assumption 1 is satisfied. Furthermore, while the complete game parameter $\theta = (\theta^{vel,1}, \theta^{v,1}, \theta^{vel,2}, \theta^{v,2},)$ is not identifiable in general, if $\theta^{vel,i}, i = 1, 2$ is constant, then $(\theta^{v,1}, \theta^{v,2})$ is identifiable from y on the pre-image of the interior of \tilde{A}_k , for any k .*

Proof of Proposition 2.

Common-coupled game. It is directly clear from the form of the utilities in Scenario 2, that this forms a common-coupled game.

Strict concavity of the potential function. Consider all subspaces \tilde{A}_k where agent 1 is faster, i.e., $a_1 > a_2$. Note that this can be one or two subspaces: if $y_1^0 > y_2^0$, then it is one subspace, but otherwise it is two (namely, where 1 or 2 reaches the intersection first, respectively).

On any one of these subspaces, the following holds true:

Regarding the distance-based term, observe that

$$\arg \min_{t \in [0, T]} |t \cdot a^1 + z^1| + |t \cdot a^2 + z^2| = -\frac{z^1}{a^1}. \quad (12)$$

To see this, observe that the argmin is given by t where agent 1 reaches the intersection, i.e, t where $t \cdot a^1 + z^1 = 0$, i.e., $t = -\frac{z^1}{a^1}$. (And this holds regardless of whether 1 or 2 first reaches the intersection.)

To see this in turn, first consider the case that agent 1 first reaches the intersection. Then, before this t , both terms are bigger (both agents are further away from the origin), while at this t , the first term is 0, and after it the left term grows faster (because the agent is faster) than the right term decreases (until the right term hits 0 as well and then also increases again).

Second, consider the case where agent 2 first reaches the intersection (in case this happens at all – i.e., if 2 starts so much closer to the origin to make this possible). Then, before 2 reaches the intersection: obviously both terms are bigger than when 2 reaches the intersection. Between 2 reaching the

intersection and 1 reaching the intersection: in this time span, the right term grows slower than the left term decreases, therefore the minimum (for this time span) happens when 1 reaches the intersection. Now after 1 has reached the intersection obviously both terms just grow.

Therefore,

$$u_T^{\text{com},\theta}(y_{[0,T]}) = -\frac{1}{a^1} \max_{t \in [0,T]} \frac{1}{\|(0, t \cdot a^1 + z^1) - (t \cdot a^2 + z^2, 0)\|_1} \quad (13)$$

$$= -\frac{1}{a^1} \max_{t \in [0,T]} \frac{1}{|t \cdot a^1 + z^1| + |t \cdot a^2 + z^2|} \quad (14)$$

$$= -\frac{1}{a^1} \frac{1}{\left| -\frac{z^1}{a^1} \cdot a^1 + z^1 \right| + \left| -\frac{z^1}{a^1} \cdot a^2 + z^2 \right|} \quad (15)$$

$$= -\frac{1}{a^1} \frac{1}{\left| -\frac{z^1}{a^1} \cdot a^2 + z^2 \right|} \quad (16)$$

$$= -\frac{1}{|z^2 a^1 - z^1 a^2|} \quad (17)$$

Keep in mind that for agent i , the time when it reaches the intersection is given by $t_i = -\frac{z^i}{a^i}$. Now, if, for the subspace under consideration, agent 1 first reaches the intersection, i.e., $-\frac{z^1}{a^1} > -\frac{z^2}{a^2}$, i.e., $\frac{z^1}{a^1} < \frac{z^2}{a^2}$, i.e., $z^1 a^2 < z^2 a^1$. Then (17) becomes $-\frac{1}{z^2 a^1 - z^1 a^2}$, which is obviously concave. Similarly for the case that agent 2 first reaches the intersection.

Regarding the velocity terms, obviously their sum is strictly concave.

So the sum of all terms is strictly concave.

Linearity and compactness of constraints. The constraints are all of the form $a_1 \geq a_2 + \varepsilon$ or $z^1 a^2 < z^2 a^1$, i.e., linear.

Identifiability. Obviously the full θ cannot be identifiable because there are no (local) diffeomorphisms between spaces of differing dimension.

Keep in mind that the parametrization from a to y is injective, so we just need to show identifiability from a . That is, we have to show that g_k is invertible on $g_k^{-1}(\text{int}(\bigcup_k \tilde{A}_k))$, where $\text{int}(\cdot)$ denotes the interior.

Since we fixed $\theta^{\text{vel},i}$, $i = 1, 2$, consider them as constants, and for what follows, for simplicity let θ stand for $(\theta^{v,1}, \theta^{v,2})$.

W.l.o.g. (the other cases work similarly) assume \tilde{A}_k is the subspace where agent 1 is faster and first reaches the intersection, so the potential function becomes

$$\psi(\theta, a) = \frac{1}{z^2 a^1 - z^1 a^2} - \theta^{\text{vel},1} (a^1 - \theta^{v,1})^2 - \theta^{\text{vel},2} (a^2 - \theta^{v,2})^2. \quad (18)$$

Now let a be such that $a = g_k(\theta)$ for some θ . We have to show that there can only be one such θ . To see this, note that a is a local NE, and thus

$$0 = \nabla_a \psi(\theta, a) = \left((-1)^{i-1} \frac{z^{3-i}}{(z^2 a^1 - z^1 a^2)^2} + 2\theta^{\text{vel},i} a^i - 2\theta^{\text{vel},i} \theta^{v,i} \right)_{i=1,2}. \quad (19)$$

But this implies

$$\theta^{v,i} = \frac{(-1)^{i-1} \frac{z^{3-i}}{(z^2 a^1 - z^1 a^2)^2} - 2\theta^{\text{vel},i} a^i}{2\theta^{\text{vel},i}}. \quad (20)$$

□



Figure 4: For the new highway data set published alongside this paper, this is roughly the recorded highway section (only the lower lane, incl. exit/entry). Note that the recorded section is in fact slightly more to the right than the picture indicates.



Figure 5: This is a zoom-in on roughly the sub-part of the highway section in Fig. 4 that is relevant for the on-ramp merging trajectories used in the experiment.

Algorithm 1: Part of preference revelation net of TGL-P that outputs the desired velocity game parameters $\theta^{v,2}, \theta^{v,1}$ and differs compared to TGL

Input: `old_vx_other, old_vx_merger` // velocities along x-axis at the last step of the past trajectory x , where ‘merger’ is the on-ramp car, and ‘other’ is the highway car

`desired_vx_other, desired_vx_merger` // output $\theta^{v,2}, \theta^{v,1}$ of TGL’s original preference revelation net

`merger_in_front` // most probable subspace given by equilibrium refinement/weighting net, whether merger merges before or after other

`big_change` // parameter - factor for allowed big change, for the experiment we used `big_change = 1.2`

`small_change` // parameter - factor for allowed small change, for the experiment we used `small_change = 1.04`

Output: `new_vx_other, new_vx_merger` // new desired velocity game parameters $\theta^{v,2}, \theta^{v,1}$

```

if merger_in_front == 0 then
  // if the highway vehicle is in front
  // clamp change of highway vehicle desired speed
  new_vx_other = clamp(desired_vx_other, old_vx_other / small_change,
    old_vx_other * small_change)
  // only allow accelerating merger vehicle, but limit maximum speed change
  new_vx_merger = clamp(desired_vx_merger, old_vx_merger, old_vx_merger * big_change)
else
  // if the merger vehicle is in front
  // clamp desired merger velocity to make it coherent with driving in front of
  // other
  new_vx_merger = clamp(desired_vx_merger, min( old_vx_merger * big_change,
    old_vx_other / big_change), old_vx_merger * big_change)
  // also clamp the desired speed of the other, distinguishing between two cases:
  if new_vx_merger > old_vx_other then
    new_vx_other = clamp(desired_vx_other, old_vx_other / small_change,
      old_vx_other * small_change)
  else
    new_vx_other = clamp(desired_vx_other, old_vx_other / big_change, old_vx_other)

```

B Experiments – further details

B.1 More detailed description of TGL-P

Let us give further details on our method *TGL-P*, that was only briefly introduced in Sec. 5.1. This method is the same as TGL described in Sec. 5.1 (building on Scenario 1), except that we modified the preference revelation net based on plausible reasoning and using parts of the equilibrium refinement/weighting net. Note that *this is still a special case of our general architecture (Sec. 3.2) in the rigorous sense*, just with a preference revelation net that incorporates a fair amount of additional reasoning and shares some structure with the equilibrium refinement net.

There are two reasons why we introduce TGL-P: First, the preference revelation net has to be trained together with the local game solver implicit layer. This means that training takes comparably long (we have an outer and an inner optimization loop, as described in Sec. 3.2). And one particular problem we experienced and have not fully solved yet, is that often the preference revelation net already starts overfitting while the game parameters that are learned “globally”, i.e., not inferred from the past trajectory by the preference revelation net, are not properly learned yet. Now TGL-P allows to demonstrate what we believe TGL itself can also achieve once the mentioned problems are overcome; in particular, it shows that the *game model class* (Γ_θ) has a substantial capacity to resemble the future trajectories. Second, TGL-P shows how the intermediate representation θ can be inspected and high level knowledge/reasoning about agents’ preferences/utilities and behavior can be incorporated.

Data set	Horizon	TGL (ours)	TGL-P (ours)	CS-LSTM [10]
highD [21]	1s	0.5	0.5	1.4
	2s	1.2	1.0	2.4
	3s	2.1	1.6	3.7
	4s	3.3	2.3	4.8
	5s	4.7	3.2	6.0
	6s	6.3	4.2	7.0
	7s	8.1	5.3	10.1
New data set (Sec. 5.1)	1s	0.9	0.9	0.8
	2s	1.7	1.7	1.6
	3s	2.6	2.6	2.3
	4s	3.6	3.5	3.3
	5s	4.6	4.3	4.4
	6s	5.9	5.2	5.3
	7s	7.3	6.2	7.2

Table 2: Mean absolute error (MAE) for all prediction horizons for all methods.

Data set	Horizon	TGL (ours)	TGL-P (ours)	CS-LSTM [10]
highD [21]	1s	0.6	0.5	1.8
	2s	1.6	1.2	3.2
	3s	3.0	2.0	5.0
	4s	4.7	3.1	6.3
	5s	6.8	4.4	7.7
	6s	9.2	5.9	9.1
	7s	12.0	7.7	14.5
New data set (Sec. 5.1)	1s	1.3	1.3	0.9
	2s	2.5	2.6	2.0
	3s	3.6	3.7	2.8
	4s	4.8	4.9	4.0
	5s	6.1	6.1	5.1
	6s	7.7	7.4	6.5
	7s	9.5	8.8	8.7

Table 3: Root mean square error (RMSE) for all prediction horizons for all methods.

Specifically, TGL-P can be described as being the same as TGL, except that the part of preference revelation net of TGL that outputs $\theta^{v,2}, \theta^{v,1}$ is replaced by Algorithm 1 (on page 15). The function $clamp(\cdot)$ is, as usual, defined by

$$clamp(z, m, M) = \max(m, \min(z, M)),$$

i.e., clipping values to m / M if they are below / above. While the details of the algorithm may look complex, the main idea is simple: we clip the outputs of the preference revelation net if they are too far off compared to what one would expect given initial velocities and output of the equilibrium refinement/weighing net. The algorithm has two parameters *big_change* and *small_change*, for which we used the values 1.2 and 1.04, respectively, in the experiment.

Note that, while in general, the equilibrium refinement/weighing net and the preference revelation net serve separate purposes, the reason why in TGL-P we share structure between them is mainly a pragmatic one: the equilibrium refinement/weighing net *can* be trained separately from the implicit layer and thus much faster – and we made the experience that it learns a reliable signal to predict the future (subspaces / selected equilibria).

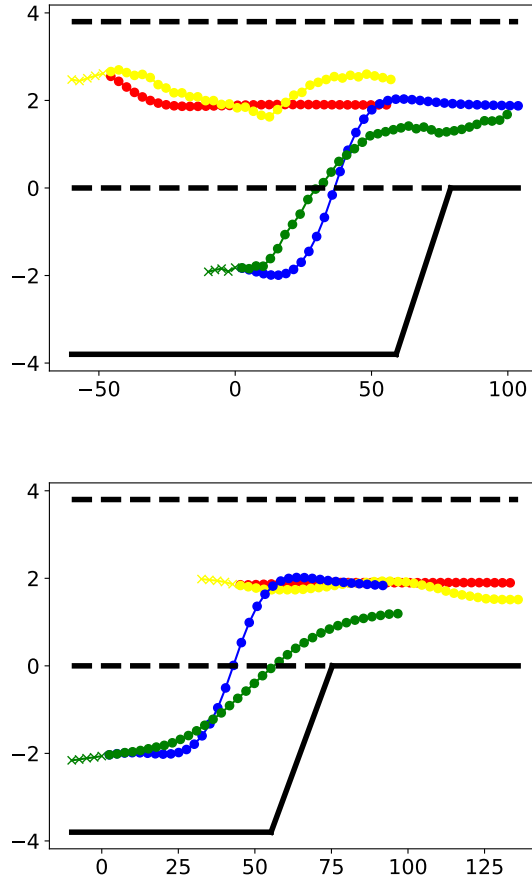


Figure 6: Example joint trajectories on *highD* data set (top) and *our new highway data set* (bottom). The *ground truth future* y is green and yellow for on-ramp and highway car, respectively, with the past trajectory segment x (at the very beginning) depicted by 'x' markers. The *prediction* \hat{y} (*most likely mode*) of our method *TGL-P* is in green and red, respectively. Note that x- and y-axis are in meters; in particular, the x-axis is significantly squeezed.

B.2 Additional details on new highway data set

One of the data sets we used in the experiment is a new one (introduced in Sec. 5.1). The full recorded highway section is roughly as the lower lane (incl. exit/entry) in Fig. 4 (on page 14) (the recorded section is in fact slightly more to the right than the picture indicates). For the experiments we focused on merging scene trajectories, which roughly take place within the smaller highway section depicted in Fig. 5 (on page 14). Note that the images in Fig. 1 are a stylized (significantly squashed in the x-dimension) version of Fig. 5.

Note that the recorded highway section in our data set – length $\sim 600\text{m}$ – is longer compared to the one section with an on-ramp in *highD*. But *highD* also contains other highway sections, and is potentially less noisy than our data set.

B.3 More details on experimental results

In the main text we only gave results averaged over all prediction horizons. Here, Tables 2, 3 (on page 16) give the results – MAE and RMSE for all methods – for *each prediction horizon individually*, from 1s to 7s.

Additionally, in Fig. 6 (on page 17) we show example joint trajectories on highD data set and our new highway data set: the past trajectory x , the prediction \hat{y} (most likely mode) of our method TGL-P, and the ground truth future trajectory y . Note that the x -axis is *significantly squeezed* in these figures.

C Remarks on rationality, local Nash equilibria, equilibrium selection, etc.

Let us make some high level remarks.

- As a remark on the (local) rationality principle in our model: We do not think that humans are perfectly instrumentally rational (i.e., strategic utility maximizers) in general, and in many multiagent trajectory settings *bounded* rationality and other phenomena may play an important role. Nonetheless, we believe that instrumental rationality is *reasonably good approximation* in many settings. And of course, game-theoretic rationality has the advantage that there is an elegant theory for it.
- In fact we use the *local* Nash equilibrium, which can also be seen as a bounded form of rationality. However, we feel that it can often be a better, more advanced approximation (to reality and/or rationality) than other concepts like level-k game theory [42]. In particular, we found it interesting that the local Nash equilibria can in fact correspond to intuitive *modes* of the joint trajectories, like which car goes first in Fig. 1. A reason for this may be that, while there may be one perfect solution (say a global Nash), due to errors and stochasticity of the environment the agents may be perturbed towards ending up at a state where a previously local Nash equilibrium may in fact now be a global Nash equilibrium.
- The problem of equilibrium selection mentioned in the main text may be seen as a form of *incompleteness* of game theory – it cannot always make a unique prediction (or prescription). Our equilibrium refinement and weighing nets can be seen as a data-driven approach to fill this incompleteness. An interesting question in this context is whether the missing information is actually contained in the preferences of the agents, or if there is additional (hidden) information required to find the unique solution/prediction.

References

- [1]
- [2] A. Alahi, K. Goel, V. Ramanathan, A. Robicquet, L. Fei-Fei, and S. Savarese. Social lstm: Human trajectory prediction in crowded spaces. In *Proceedings of the IEEE conference on computer vision and pattern recognition*, pages 961–971, 2016.
- [3] B. Amos and J. Z. Kolter. Optnet: Differentiable optimization as a layer in neural networks. In *Proceedings of the 34th International Conference on Machine Learning-Volume 70*, pages 136–145. JMLR. org, 2017.
- [4] S. Bai, J. Z. Kolter, and V. Koltun. Deep equilibrium models. In *Advances in Neural Information Processing Systems*, pages 688–699, 2019.
- [5] D. Balduzzi, S. Racaniere, J. Martens, J. Foerster, K. Tuyls, and T. Graepel. The mechanics of n-player differentiable games. *arXiv preprint arXiv:1802.05642*, 2018.
- [6] C. Blaiotta. Learning generative socially aware models of pedestrian motion. *IEEE Robotics and Automation Letters*, 4(4):3433–3440, 2019.
- [7] S. Boyd, S. P. Boyd, and L. Vandenberghe. *Convex optimization*. Cambridge university press, 2004.
- [8] F. Camara, R. Romano, G. Markkula, R. Madigan, N. Merat, and C. Fox. Empirical game theory of pedestrian interaction for autonomous vehicles. In *Proceedings of Measuring Behavior 2018*. Manchester Metropolitan University, 2018.
- [9] T. Q. Chen, Y. Rubanova, J. Bettencourt, and D. K. Duvenaud. Neural ordinary differential equations. In *Advances in neural information processing systems*, pages 6571–6583, 2018.

- [10] N. Deo and M. M. Trivedi. Convolutional social pooling for vehicle trajectory prediction. In *Proceedings of the IEEE Conference on Computer Vision and Pattern Recognition Workshops*, pages 1468–1476, 2018.
- [11] L. El Ghaoui, F. Gu, B. Travacca, and A. Askari. Implicit deep learning. *arXiv preprint arXiv:1908.06315*, 2019.
- [12] J. F. Fisac, E. Bronstein, E. Stefansson, D. Sadigh, S. S. Sastry, and A. D. Dragan. Hierarchical game-theoretic planning for autonomous vehicles. In *2019 International Conference on Robotics and Automation (ICRA)*, pages 9590–9596. IEEE, 2019.
- [13] C. Fox, F. Camara, G. Markkula, R. Romano, R. Madigan, N. Merat, et al. When should the chicken cross the road?: Game theory for autonomous vehicle-human interactions. 2018.
- [14] A. Gupta, J. Johnson, L. Fei-Fei, S. Savarese, and A. Alahi. Social GAN: Socially acceptable trajectories with generative adversarial networks. In *Proceedings of the IEEE Conference on Computer Vision and Pattern Recognition*, pages 2255–2264, 2018.
- [15] J. C. Harsanyi, R. Selten, et al. *A general theory of equilibrium selection in games*, volume 1. The MIT Press, 1988.
- [16] J. S. Hartford, J. R. Wright, and K. Leyton-Brown. Deep learning for predicting human strategic behavior. In *Advances in Neural Information Processing Systems*, pages 2424–2432, 2016.
- [17] D. Helbing and P. Molnar. Social force model for pedestrian dynamics. *Physical review E*, 51(5):4282, 1995.
- [18] K. Kang and H. A. Rakha. Game theoretical approach to model decision making for merging maneuvers at freeway on-ramps. *Transportation Research Record*, 2623(1):19–28, 2017.
- [19] H. Kita. A merging–giveaway interaction model of cars in a merging section: a game theoretic analysis. *Transportation Research Part A: Policy and Practice*, 33(3-4):305–312, 1999.
- [20] H. Kita, K. Tanimoto, and K. Fukuyama. A game theoretic analysis of merging-giveaway interaction: a joint estimation model. *Transportation and Traffic Theory in the 21st Century*, pages 503–518, 2002.
- [21] R. Krajewski, J. Bock, L. Kloeker, and L. Eckstein. The highD Dataset: A Drone Dataset of Naturalistic Vehicle Trajectories on German Highways for Validation of Highly Automated Driving Systems. In *2018 IEEE 21st International Conference on Intelligent Transportation Systems (ITSC)*, 2018.
- [22] M. Kuderer, H. Kretschmar, C. Sprunk, and W. Burgard. Feature-based prediction of trajectories for socially compliant navigation. In *Robotics: science and systems*, 2012.
- [23] N. Li, I. Kolmanovsky, A. Girard, and Y. Yildiz. Game theoretic modeling of vehicle interactions at unsignalized intersections and application to autonomous vehicle control. In *2018 Annual American Control Conference (ACC)*, pages 3215–3220. IEEE, 2018.
- [24] Y. Li and H. Liu. Implementation of stochastic quasi-newton’s method in pytorch. *arXiv preprint arXiv:1805.02338*, 2018.
- [25] C. K. Ling, F. Fang, and J. Z. Kolter. What game are we playing? End-to-end learning in normal and extensive form games. In *IJCAI-ECAI-18: The 27th International Joint Conference on Artificial Intelligence and the 23rd European Conference on Artificial Intelligence*, 2018.
- [26] C. K. Ling, F. Fang, and J. Z. Kolter. Large scale learning of agent rationality in two-player zero-sum games. In *Proceedings of the AAAI Conference on Artificial Intelligence*, volume 33, pages 6104–6111, 2019.
- [27] H. X. Liu, W. Xin, Z. Adam, and J. Ban. A game theoretical approach for modelling merging and yielding behaviour at freeway on-ramp sections. *Transportation and traffic theory*, 3: 197–211, 2007.

- [28] W.-C. Ma, D.-A. Huang, N. Lee, and K. M. Kitani. Forecasting interactive dynamics of pedestrians with fictitious play. In *Proceedings of the IEEE Conference on Computer Vision and Pattern Recognition*, pages 774–782, 2017.
- [29] D. Monderer and L. S. Shapley. Potential games. *Games and economic behavior*, 14(1): 124–143, 1996.
- [30] N. Nisan, T. Roughgarden, E. Tardos, and V. V. Vazirani. *Algorithmic game theory*, volume 1. Cambridge University Press Cambridge, 2007.
- [31] M. J. Osborne and A. Rubinstein. *A course in game theory*. MIT press, 1994.
- [32] L. Peters, D. Fridovich-Keil, C. J. Tomlin, and Z. N. Sunberg. Inference-based strategy alignment for general-sum differential games. *arXiv preprint arXiv:2002.04354*, 2020.
- [33] L. J. Ratliff, S. A. Burden, and S. S. Sastry. Characterization and computation of local Nash equilibria in continuous games. In *2013 51st Annual Allerton Conference on Communication, Control, and Computing (Allerton)*, pages 917–924. IEEE, 2013.
- [34] L. J. Ratliff, S. A. Burden, and S. S. Sastry. On the characterization of local Nash equilibria in continuous games. *IEEE Transactions on Automatic Control*, 61(8):2301–2307, 2016.
- [35] T. S. Reddy, V. Gopikrishna, G. Zaruba, and M. Huber. Inverse reinforcement learning for decentralized non-cooperative multiagent systems. In *2012 IEEE International Conference on Systems, Man, and Cybernetics (SMC)*, pages 1930–1935. IEEE, 2012.
- [36] A. Robicquet, A. Sadeghian, A. Alahi, and S. Savarese. Learning social etiquette: Human trajectory understanding in crowded scenes. In *European conference on computer vision*, pages 549–565. Springer, 2016.
- [37] R. W. Rosenthal. A class of games possessing pure-strategy nash equilibria. *International Journal of Game Theory*, 2(1):65–67, 1973.
- [38] A. Rudenko, L. Palmieri, M. Herman, K. M. Kitani, D. M. Gavrila, and K. O. Arras. Human motion trajectory prediction: A survey. *arXiv preprint arXiv:1905.06113*, 2019.
- [39] T. Salzmann, B. Ivanovic, P. Chakravarty, and M. Pavone. Trajectron++: Multi-agent generative trajectory forecasting with heterogeneous data for control. *arXiv preprint arXiv:2001.03093*, 2020.
- [40] Y. Shoham and K. Leyton-Brown. *Multiagent systems: Algorithmic, game-theoretic, and logical foundations*. Cambridge University Press, 2008.
- [41] R. Spica, D. Falanga, E. Cristofalo, E. Montijano, D. Scaramuzza, and M. Schwager. A real-time game theoretic planner for autonomous two-player drone racing. *arXiv preprint arXiv:1801.02302*, 2018.
- [42] D. O. Stahl and P. W. Wilson. On players’ models of other players: Theory and experimental evidence. *Games and Economic Behavior*, 10(1):218–254, 1995.
- [43] L. Sun, W. Zhan, and M. Tomizuka. Probabilistic prediction of interactive driving behavior via hierarchical inverse reinforcement learning. In *2018 21st International Conference on Intelligent Transportation Systems (ITSC)*, pages 2111–2117. IEEE, 2018.
- [44] C. Tang and R. R. Salakhutdinov. Multiple futures prediction. In *Advances in Neural Information Processing Systems*, pages 15398–15408, 2019.
- [45] R. Tian, S. Li, N. Li, I. Kolmanovsky, A. Girard, and Y. Yildiz. Adaptive game-theoretic decision making for autonomous vehicle control at roundabouts. In *2018 IEEE Conference on Decision and Control (CDC)*, pages 321–326. IEEE, 2018.
- [46] X. Wang and D. Klabjan. Competitive multi-agent inverse reinforcement learning with sub-optimal demonstrations. *arXiv preprint arXiv:1801.02124*, 2018.

- [47] X. Wang, S. Ma, D. Goldfarb, and W. Liu. Stochastic quasi-newton methods for nonconvex stochastic optimization. *SIAM Journal on Optimization*, 27(2):927–956, 2017.
- [48] S. Zazo, S. V. Macua, M. Sánchez-Fernández, and J. Zazo. Dynamic potential games with constraints: Fundamentals and applications in communications. *IEEE Transactions on Signal Processing*, 64(14):3806–3821, 2016.
- [49] C. Zhang, J. Zhu, W. Wang, and J. Xi. Spatiotemporal learning of multivehicle interaction patterns in lane-change scenarios. *arXiv preprint arXiv:2003.00759*, 2020.
- [50] Q. Zhang, D. Filev, H. Tseng, S. Szwabowski, and R. Langari. Addressing mandatory lane change problem with game theoretic model predictive control and fuzzy markov chain. In *2018 Annual American Control Conference (ACC)*, pages 4764–4771. IEEE, 2018.
- [51] X. Zhang, K. Zhang, E. Miehling, and T. Basar. Non-cooperative inverse reinforcement learning. In *Advances in Neural Information Processing Systems*, pages 9482–9493, 2019.